

## Reduction of the Spin Susceptibility in the Superconducting State of $\text{Sr}_2\text{RuO}_4$ Observed by Polarized Neutron Scattering

A. N. Petsch,<sup>1,\*</sup> M. Zhu,<sup>1</sup> Mechthild Enderle,<sup>2</sup> Z. Q. Mao,<sup>3,4</sup> Y. Maeno<sup>5</sup>,<sup>3</sup> I. I. Mazin,<sup>5</sup> and S. M. Hayden<sup>1,†</sup>

<sup>1</sup>*H.H. Wills Physics Laboratory, University of Bristol, Bristol BS8 1TL, United Kingdom*

<sup>2</sup>*Institut Laue-Langevin, CS 20156, 38042 Grenoble Cedex 9, France*

<sup>3</sup>*Department of Physics, Graduate School of Science, Kyoto University, Kyoto 606-8502, Japan*

<sup>4</sup>*Department of Physics, Pennsylvania State University, University Park, Pennsylvania 16802, USA*

<sup>5</sup>*Department of Physics and Astronomy, George Mason University and Quantum Science and Engineering Center, Fairfax, Virginia 22030, USA*



(Received 7 February 2020; revised 1 July 2020; accepted 14 October 2020; published 18 November 2020)

Recent observations [A. Pustogow *et al.*, *Nature (London)* **574**, 72 (2019).] of a drop of the  $^{17}\text{O}$  nuclear magnetic resonance (NMR) Knight shift in the superconducting state of  $\text{Sr}_2\text{RuO}_4$  challenged the popular picture of a chiral odd-parity paired state in this compound. Here we use polarized neutron scattering (PNS) to show that there is a  $34 \pm 6\%$  drop in the magnetic susceptibility at the Ru site below the superconducting transition temperature. We measure at lower fields  $H \sim \frac{1}{3}H_{c2}$  than a previous PNS study allowing the suppression to be observed. The PNS measurements show a smaller susceptibility suppression than NMR measurements performed at similar field and temperature. Our results rule out the chiral odd-parity  $\mathbf{d} = \hat{z}(k_x \pm ik_y)$  state and are consistent with several recent proposals for the order parameter including even-parity  $B_{1g}$  and odd-parity helical states.

DOI: 10.1103/PhysRevLett.125.217004

**Introduction.**— $\text{Sr}_2\text{RuO}_4$  is a moderately correlated oxide metal, which forms a good Fermi liquid and superconducts [1] below 1.5 K. It has been initially proposed as a solid-state analog [2,3] of superfluid  $^3\text{He-A}$ , driven by proximity to ferromagnetism. The superconducting state was widely assumed to possess chiral odd-parity order [4,5] with broken time-reversal symmetry [6]. An important property of odd-parity (triplet-paired) superconductors is that for some magnetic field directions the spin susceptibility may show no change upon entering the superconducting state. This may be investigated by probes not sensitive to the superconducting diamagnetic screening currents, such as nuclear magnetic resonance (NMR) or polarized neutron scattering (PNS). Early studies of the susceptibility using the NMR Knight shift with  $^{17}\text{O}$  (NMR) [7] and PNS [8] detected no change while crossing the superconducting transition when magnetic fields were applied parallel to the  $\text{RuO}_2$  or  $ab$  planes. These observations supported the picture of triplet pairing with an out of plane  $\mathbf{d}$  vector or an unpinned in plane  $\mathbf{d}$  vector  $\perp \mathbf{H}$ . Muon-spin rotation [6] and Kerr effect [9] studies provide evidence that the superconducting state exhibits time-reversal symmetry breaking (TRSB).

More recently, it has become clear that it is difficult to consistently describe the physical properties of the superconducting state with a simple odd-parity representation [10]. For example, the favored  $\mathbf{d} = \hat{z}(k_x \pm ik_y)$  state implies the existence of edge currents, which are not detected experimentally [11–14], and  $H_{c2}$  is much lower than expected [10].

Also a NMR experiment failed to detect any changes in susceptibility for a  $c$ -axis field [15], even though it would have to be reduced below  $T_c$  in the  $\hat{z}(k_x \pm ik_y)$  state. It was shown that rotation of the order parameter vector would be forbidden by the strong spin-orbit coupling [16,17], which led one of us to conclude that “the Knight shift in  $\text{Sr}_2\text{RuO}_4$  remains a challenge for theorists; until this puzzle is resolved, we cannot use the Knight shift argument” [16].

A recent  $^{17}\text{O}$ -NMR study by Pustogow *et al.* [18] detected a significant reduction in the Knight shift on entering the superconducting state for in plane fields for the first time. This result has been reproduced by Ishida *et al.* [19]. The reduction in susceptibility should also be observed by PNS. However, a PNS study [8] with relatively poor statistics and at a field  $\mu_0 H = 1$  T was unable to observe a reduction.

In this Letter, we report PNS measurements at a lower field ( $\mu_0 H = 0.5$  T) and with better statistics. We find a  $34 \pm 6\%$  drop in the magnetic susceptibility at the Ru site below  $T_c$ . This is somewhat smaller than the  $63 \pm 8\%$  drop observed by NMR Knight shift measurements [19] at the in plane O site for a similar field  $\mu_0 H = 0.48$  T. The non-interacting spin susceptibility in the superconducting state extracted from our PNS measurements is larger than that determined from the NMR Knight shift [18,19]. Thus, the PNS data better match different paired states. We discuss possible reasons for the difference between the two observations and the constraints our results place on the allowed superconducting order parameter.

TABLE I. Irreducible representations of superconducting order parameters compatible with the tetragonal point group  $D_{4h}$  with strong spin-orbit coupling [23]. The left and right sides are even-parity (singlet) and odd-parity (triplet) states, respectively. Columns 3 and 10 show states with vertical ( $v$ ),  $\parallel k_z$ , or horizontal ( $h$ ),  $\perp k_z$ , line nodes on a 2D Fermi surface. States with  $k_\mu$  transform like  $\sin k_\mu$ , while states with  $k_\mu^2$  transform like  $\cos k_\mu$ . Ticks indicate TRSB.  $\chi_0$  is calculated from Eq. (2) for a cylindrical Fermi surface.

State	Basis function	Line nodes	TRSB	$\chi_0(H, T \rightarrow 0)/\chi_0(n)$ with $\mathbf{H}\parallel$			State	Basis function	Line nodes	TRSB	$\chi_0(H, T \rightarrow 0)/\chi_0(n)$ with $\mathbf{H}\parallel$		
				[100]	[110]	[001]					[100]	[110]	[001]
$A_{1g}$	$k_x^2 + k_y^2$		$\times$	0	0	0	$A_{1u}$	$\hat{x}k_x + \hat{y}k_y$		$\times$	1/2	1/2	1
								$\hat{z}k_z$	( $h$ )	$\times$	1	1	0
$A_{2g}$	$k_x k_y (k_x^2 - k_y^2)$	( $v$ )	$\times$	0	0	0	$A_{2u}$	$\hat{x}k_y - \hat{y}k_x$		$\times$	1/2	1/2	1
								$\hat{z}k_x k_y k_z (k_x^2 - k_y^2)$	( $v, h$ )	$\times$	1	1	0
$B_{1g}$	$k_x^2 - k_y^2$	( $v$ )	$\times$	0	0	0	$B_{1u}$	$\hat{x}k_x - \hat{y}k_y$		$\times$	1/2	1/2	1
								$\hat{z}k_x k_y k_z$	( $v, h$ )	$\times$	1	1	0
$B_{2g}$	$k_x k_y$	( $v$ )	$\times$	0	0	0	$B_{2u}$	$\hat{x}k_y + \hat{y}k_x$		$\times$	1/2	1/2	1
								$\hat{z}k_z (k_x^2 - k_y^2)$	( $v, h$ )	$\times$	1	1	0
$E_g(a)$	$k_x k_z; k_y k_z$	( $v, h$ )	$\times$	0	0	0	$E_u(a)$	$\hat{x}k_x; \hat{y}k_z$	( $h$ )	$\times$	0; 1	1/2	1
								$\hat{z}k_x; \hat{z}k_y$	( $v$ )	$\times$	1	1	0
$E_g(b)$	$(k_x \pm k_y)k_z$	( $v, h$ )	$\times$	0	0	0	$E_u(b)$	$(\hat{x} \pm \hat{y})k_z$	( $h$ )	$\times$	1/2	0; 1	1
								$\hat{z}(k_x \pm k_y)$	( $v$ )	$\times$	1	1	0
$E_g(c)$	$(k_x \pm ik_y)k_z$	( $h$ )	$\checkmark$	0	0	0	$E_u(c)$	$(\hat{x} \pm i\hat{y})k_z$	( $h$ )	$\checkmark$	1/2	1/2	1
								$\hat{z}(k_x \pm ik_y)$		$\checkmark$	1	1	0

The spin susceptibility as a probe of the superconducting state.—The transition to a superconducting state involves the pairing of electrons and hence a change in the spin wave function. In the case of singlet pairing, where the spin susceptibility is suppressed everywhere (barring exotic cases as Ising superconductivity), its  $T$  dependence is described by the Yosida function [20,21]. A triplet superconductor is described by a spinor order parameter,

$$\Delta = \begin{bmatrix} \Delta_{\uparrow\uparrow} & \Delta_{\uparrow\downarrow} \\ \Delta_{\downarrow\uparrow} & \Delta_{\downarrow\downarrow} \end{bmatrix} = \Delta \begin{bmatrix} -d_x + id_y & d_z \\ d_z & d_x + id_y \end{bmatrix}, \quad (1)$$

where the  $\mathbf{d}$  vector is  $\mathbf{d} = (d_x, d_y, d_z)$ . The noninteracting spin susceptibility tensor is given by [22]

$$\frac{\chi_{0,\alpha\beta}}{\chi_0(n)} = \delta_{\alpha\beta} + \int \frac{d\Omega}{4\pi} [Y(\hat{\mathbf{k}}, T) - 1] \Re \left\{ \frac{d_\alpha^*(\mathbf{k}) d_\beta(\mathbf{k})}{\mathbf{d}^*(\mathbf{k}) \cdot \mathbf{d}(\mathbf{k})} \right\}, \quad (2)$$

where the integral is over the Fermi surface,  $Y(\hat{\mathbf{k}}, T)$  is the Yosida function, and  $\chi_0(n)$  is the normal-state spin susceptibility. Table I shows  $\chi_0(T \rightarrow 0, H \rightarrow 0) = \chi_0(0)$  evaluated using Eq. (2) for selected irreducible representations and applied field directions.

The measurements of the spin susceptibility in the superconducting state are complicated by diamagnetic screening due to supercurrents, which precludes quantitative measurements with standard techniques such as

superconducting quantum interference device (SQUID) magnetometry. The NMR Knight shift and PNS have been used successfully to measure the spin susceptibility in the superconducting state. The Knight shift  $K$  originates from the hyperfine interaction between the nuclear moment and the magnetic field at the nuclear site produced by the electrons surrounding that site, which is only indirectly related to the total magnetization. For instance, core polarization and spin-dipole interaction do not contribute to the latter, but affect the Knight shift, while spin and orbital moments have different spatial distributions and therefore produce different contributions to  $K$  with opposite signs in some cases [24,25]. In contrast, PNS probes the total magnetization density  $M(\mathbf{r})$  induced by an external magnetic field  $\mu_0 H$ . The orbital and spin magnetization are equally weighted and  $M(\mathbf{r})$  is averaged in space. In the normal state of  $\text{Sr}_2\text{RuO}_4$ , three bands cross the Fermi surface [26]. The partially filled Ru  $t_{2g}$  orbitals account for the majority of the density of states at the Fermi energy. Hence, the majority of the spin susceptibility is associated with the Ru site probed by PNS.

In PNS, the spatially varying density  $M(\mathbf{r})$  is measured by diffraction. This technique was first applied to  $\text{V}_3\text{Si}$  by Shull and Wedgwood [27]. It has also been used to probe cuprate [28] and iron-based [29,30] superconductors where singlet pairing has been observed. Early PNS measurements by Shull and Wedgwood [27] of the  $T$  dependence of the induced magnetization in  $\text{V}_3\text{Si}$  showed that the

susceptibility only dropped to about  $\frac{1}{3}$  of its normal-state value for applied fields of  $\approx 0.1H_{c2}$ . This residual susceptibility is due to the orbital susceptibility present in transition metals [31,32]. Importantly, such cancellation effects work very differently in NMR and PNS, for instance, in V metal NMR shows no or a very small change [33,34] in the Knight shift across  $T_c$ , because of nearly exact cancellation of the core polarization (an effect specific to NMR) and the Fermi-contact term.

NMR and PNS probe the susceptibility in a superconductor in the mixed state and typically in relatively high magnetic fields  $\sim 1$  T. It is well known that vortices create low-energy electronic states [35,36]. In the mixed state of conventional superconductors, the associated quasiparticle density of states  $\mathcal{N}_F^*(H) \propto \mathcal{N}_F^*(n)H/H_{c2}$  comes from low-energy localized states in the vortex cores [35], while in superconductors with lines of gap nodes  $\mathcal{N}_F^*(H) \propto \mathcal{N}_F^*(n)\sqrt{H/H_{c2}}$  comes from the vicinity of the gap nodes in the momentum space and partially from outside the vortex cores [36]. The same states give rise to a linear heat capacity and also contribute to the spin susceptibility. For example, a linear field dependence of  $\chi = M/H$  has been observed [29] in the superconducting state of  $\text{Ba}(\text{Fe}_{1-x}\text{Co}_x)_2\text{As}_2$ .

*Experimental method.*—The experimental setup and crystal were the same as described in Duffy *et al.* [8]. A single crystal (C117) of  $\text{Sr}_2\text{RuO}_4$  with dimensions of  $1.5 \times 2 \times 5$  mm grown by the floating-zone method was mounted with [100] vertical. The sample size was chosen so as not to saturate the detector.  $T_c$  of this sample is 1.47 K and  $\mu_0 H_{c2}(100 \text{ mK}) = 1.43$  T for  $\mathbf{H} \parallel [110]$  [8,37]. We used the three-axis spectrometer IN20 at the Institut Laue-Langevin, Grenoble [38]. A vertical magnetic field was applied perpendicular to the scattering plane along the [100] direction. Measurements of the nuclear Bragg reflections (002) and (011) verified that the field was within  $0.11^\circ$  of the [100] direction. The PNS experiments were performed in the superconducting state at the (011) Bragg reflection with  $\mu_0 H = 0.5$  T. The beam was monochromatic with  $E = 63$  meV. The spectrometer beam polarization was  $93.2 \pm 0.1\%$ , measured at the (011) reflection using a Heusler monochromator and analyzer. Detector counts were normalized either to time or by using a neutron counter placed in the incident beam. Both methods produced consistent results. The sample was field cooled, and test measurements with polarization analysis were performed to check for depolarization from the vortex lattice. We measured the beam polarization at the (002) and (011) Bragg reflections for  $\mu_0 H = 0.5$  T, and no measurable difference between superconducting and normal states could be detected. Susceptibility measurements were performed with a polarized beam without the analyzer as in Duffy *et al.* [8].

PNS experiments [8,29] can directly probe the real-space magnetization density  $\mathbf{M}(\mathbf{r})$  in the unit cell, induced by a large magnetic field  $\mu_0 H$ . Because of the periodic crystal

structure, the applied magnetic field induces a magnetization density with spatial Fourier components  $\mathbf{M}(\mathbf{G})$ , where  $\mathbf{G}$  are the reciprocal lattice vectors, and

$$\mathbf{M}(\mathbf{G}) = \int_{\text{unit cell}} \mathbf{M}(\mathbf{r}) \exp(i\mathbf{G} \cdot \mathbf{r}) d\mathbf{r}. \quad (3)$$

We measure the flipping ratio  $R$ , defined as the ratio of the cross sections  $I_+$ ,  $I_-$  of polarized incident beams with neutrons parallel or antiparallel to the applied magnetic field. A detector insensitive to the scattered spin polarization and summing over the final spin states was used. The experiment is carried out in the limit  $(\gamma r_0/2\mu_B)M(\mathbf{G})/F_N(\mathbf{G}) \ll 1$ . In this limit [8], the flipping ratio is

$$R = 1 - \frac{2\gamma r_0}{\mu_B} \frac{M(\mathbf{G})}{F_N(\mathbf{G})}, \quad (4)$$

where the nuclear structure factor  $F_N(\mathbf{G})$  is known from the crystal structure and  $\gamma r_0 = 5.36 \times 10^{-15}$  m. For the (011) reflection, we used  $F_N = 4.63 \times 10^{-15}$  m.f.u. $^{-1}$ .

*Results.*—In the present experiment we apply magnetic fields along the [100] direction to allow comparison with NMR measurements [18,19]. We first established the normal-state susceptibility  $\chi(n)$  by making measurements at  $T = 1.5$  K and  $\mu_0 H = 2.5$  T as shown in Fig. 1(a). Our signal,  $1 - R$ , is proportional to the induced moment [Eq. (4)] and our error bars are determined by the number of counts in  $I_{\pm}$  and hence the counting time. Thus, the 2.5 T measurement (closed diamond) provides the most accurate estimate of the normal-state susceptibility, shown by the horizontal solid line. The data have been converted to  $\chi$  using Eq. (4) [39]. A further measurement (closed circle) was performed in the superconducting state at  $T = 0.06$  K and  $\mu_0 H = 0.5$  T with a total counting time of 52 h in order to obtain good statistics and a small error bar. The difference between  $\chi(n)$  and the  $\chi(T = 0.06 \text{ K}, \mu_0 H = 0.5 \text{ T})$  point demonstrates a clear drop in  $\chi$  of  $34 \pm 6\%$  on entering the superconducting state.

Figure 1(b) shows PNS and NMR results presented as a function of magnetic field. It is notable that PNS yields a larger susceptibility in the superconducting state than what can be deduced from the  $^{17}\text{O}$  Knight shift [19]  $K$  at comparable field and temperature. Specifically, at  $\mu_0 H \approx 0.5$  T and  $T \approx 60$  mK, we have  $\chi(\text{PNS})/\chi(n) = 0.66 \pm 0.06$  and  $K(\text{NMR})/K(n) = 0.37 \pm 0.08$ . In the Supplemental Material [42], we show how the measured susceptibility  $\chi$  is corrected for Fermi liquid effects (Stoner enhancement) and the orbital contribution. The corrected noninteracting spin susceptibility  $\chi_0/\chi_0(n)$ , which can be compared with theory, is shown in Fig. 1(c).

As discussed above, PNS and NMR probe the magnetization in different ways, so there are reasons why the results may be different. For the (011) Bragg reflection, the PNS

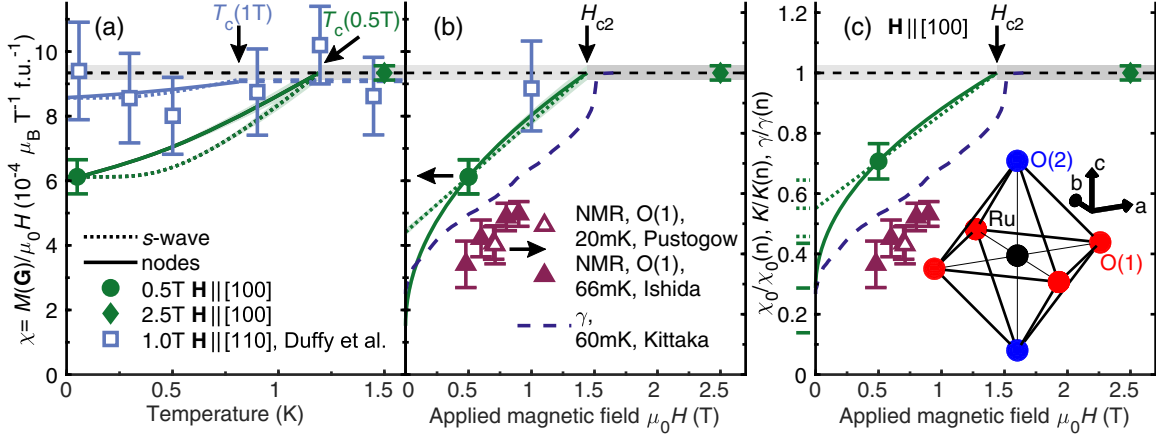


FIG. 1. PNS measurements of  $\chi = M(\mathbf{G})/H$  at  $\mathbf{G} = (011)$ . (a)  $T$  dependence of  $\chi$  shows a drop below  $T_c$  for  $\mu_0 \mathbf{H} \parallel [100]$ . Results of Duffy *et al.* [8] with  $\mu_0 \mathbf{H} = 1\text{T} \parallel [110]$  (open symbols) are scaled by the Ru magnetic form factor [40].  $T$  dependencies (dotted and solid lines) are fitted using the Yosida functions [20,21,41]. (b)  $H$  dependence of  $\chi$  at  $T = 60$  mK.  $\chi(H)$  is fitted to  $s$ -wave and nodal models (see text). Blue square is from fit [42] in (a). (c)  $H$  dependence of the scaled noninteracting spin susceptibility  $\chi_0(H)/\chi_0(n)$  determined by correction for Stoner enhancement and orbital contribution [42]. Also shown are  $^{17}\text{O}$  NMR Knight shift  $K$ , data at similar temperatures from Pustogow *et al.* [18] and Ishida *et al.* [19], and the measured linear coefficient of the specific heat  $\gamma = C_e/T$  from Kittaka *et al.* [43]. Both quantities have been scaled to their normal-state values. Bars to the right of (c) show intercepts of model curves and confidence intervals.

method measures  $M[\mathbf{G} = (011)] \approx M_{\text{Ru}} \times f_{\text{Ru}}(\mathbf{G}) + 1.04 \times M_{\text{O}(2)} \times f_{\text{O}(2)}(\mathbf{G}) \approx M_{\text{Ru}} \times f_{\text{Ru}}(\mathbf{G})$ , where  $f$  is the magnetic form factor and  $M$  is the magnetic moment on a given site. Note that the O(1) oxygen sites [see Fig. 1(c)] do not contribute to the magnetic signal observed at this reflection. Further, the moment on the oxygen O(2) sites is known to be small from NMR Knight shift measurements [19] and density-functional theory calculations [55,56]. Thus, our measurement is essentially sensitive only to the Ru sites where most of the moment resides. In contrast, recent NMR experiments [18,19] mainly probed the oxygen O(1) sites.

As mentioned,  $\chi_0(T)$  for an isotropic  $s$ -wave superconductor is expected to follow the Yosida function [20]. This function can be easily modified [21] to account for a superconductor with vertical line nodes. At low temperatures, the drop in  $\chi \equiv M/H$  will be field dependent due to the introduction of vortices. Modeling the effect of vortices on the spin susceptibility is theoretically difficult; in addition,  $\text{Sr}_2\text{RuO}_4$  shows a first-order phase transition at  $H_{c2}$  with a “step” in the spin magnetization [57–59]. Nevertheless, in Fig. 1(c) we fit two simple illustrative low- $T$  field dependencies of  $\chi_0(H)$  with  $\chi_{0,s}(H) = \chi_0(0) + \Delta\chi H/H_{c2}$  and  $\chi_{0,nodal}(H) = \chi_0(0) + \Delta\chi \sqrt{H/H_{c2}}$  for the  $s$ -wave and nodal cases using the actual  $H_{c2}$  [35,36]. Our  $s$ -wave and nodal field-dependent fits yield zero-field residual values of  $\chi_0(0)/\chi_0(n)$  of  $0.55 \pm 0.09$  and  $0.29 \pm 0.15$ , respectively. Both fits give  $\chi \approx 8 \times 10^{-4} \mu_B T^{-1} \text{ f.u.}^{-1}$  for  $\mu_0 H = 1$  T.

Our data are consistent with two interesting scenarios as  $H \rightarrow 0$ : (i) a rapid reduction of  $\chi_0$  below  $\frac{1}{3}H_{c2}$  [solid line in Fig. 1(c)] and (ii) a large residual contribution to  $\chi_0$  in the  $H \rightarrow 0$  limit (dotted line). Case (i) would be consistent with

an even-parity (singlet) state with deep minima or nodes [36] in the gap and a small residual spin susceptibility. In case (ii), there would be a large residual spin susceptibility. This would be qualitatively consistent with various states in Table I and other proposals discussed below.

Both  $\chi_0(H)$  and the linear coefficient of specific heat  $\gamma(H) = C_e/T$  can detect the low-energy states introduced by vortices. For a singlet superconductor, they are expected to show similar behavior [59]. In Figs. 1(b) and 1(c), we reproduce the measured  $\gamma(H)$  [43] for  $\mathbf{H} \parallel [100]$  and the recent NMR Knight shift [18,19], which both yield smaller values when normalized to the normal state [42].

It is instructive to compare the present PNS data with that of Duffy *et al.* [8] measured with  $\mathbf{H} \parallel [110]$ . From Table I, one can see that the effect of the field is expected to be the same for the [100] and [110] directions for all order parameter symmetries, except for two of the  $E_u$  states. In Fig. 1(a), we also show the PNS results of Duffy *et al.* [8] (open squares) measured at a field of 1 T with  $\mathbf{H} \parallel [110]$ . These were probed at the (002) Bragg peak and have therefore been scaled by the ratio of the Ru form factors [40,60] at (011) and (002) for comparison. The blue solid and dotted lines show  $T$ -dependent fits (See Supplemental Material [42]) of a Yosida functions [20,21]. When the data are fitted in this way, the resulting 1 T susceptibility point has a large error bar [Fig. 1(b)]. Thus, Duffy *et al.* [8] were probably unable to resolve a change in  $\chi$  below  $T_c$  because of the lower statistical accuracy and use of a higher field, where the suppression effect is smaller. However, the  $E_u$  state  $\mathbf{d} = (\hat{x} - \hat{y})k_z$  (which shows no change in  $\chi_0$  for  $\mathbf{H} \parallel [110]$  and a change for  $\mathbf{H} \parallel [100]$ ) cannot currently be ruled out by the PNS experiments.

*Discussion.*—Many superconducting states have been proposed for  $\text{Sr}_2\text{RuO}_4$ . Some of those are shown in Table I and, following the observations of Pustogow *et al.* [18], there have also been new theoretical proposals [61–63]. The PNS measurements reported here yield a noninteracting spin susceptibility in the superconducting state  $\chi_0(\mu_0 H = 0.5\text{T})/\chi_0(n) = 0.71 \pm 0.06$ , which is larger than the NMR Knight shift [18,19]. Thus, the PNS data better match different states. We concluded above that the residual  $\chi_0(0)/\chi_0(n) = 0.55 \pm 0.09$  or  $0.29 \pm 0.15$  for non-nodal [e.g.,  $\hat{\mathbf{x}}k_x + \hat{\mathbf{y}}k_y$ ,  $\hat{\mathbf{z}}(k_x \pm ik_y)$ ] or (near) nodal [e.g.,  $s'$ ,  $d_{x^2-y^2}$ ,  $(k_x \pm ik_y)k_z$ ] gaps, respectively. Thus, our PNS measurements do not rule out all odd-parity states, but they do rule out those with  $\chi_0(0)/\chi_0(n) = 1$  in Table I. This includes the previously widely considered chiral  $p$ -wave  $\mathbf{d} = \hat{\mathbf{z}}(k_x \pm ik_y)$  state [2,4,5,64]. Odd-parity states with in plane  $\mathbf{d}$  vectors such as the helical triplet (e.g.,  $\mathbf{d} = \hat{\mathbf{x}}k_x + \hat{\mathbf{y}}k_y$ ) states proposed by Rømer *et al.* [61] have a partial ( $\approx 50\%$ ) suppression of  $\chi_s$  and therefore are not ruled out. Other states that are qualitatively compatible with our observations include the TRSB  $s' + id_{x^2-y^2}$  and nonunitary  $\hat{\mathbf{x}}k_x \pm i\hat{\mathbf{y}}k_y$  states [61] proposed by Rømer *et al.* [61], states resulting from the 3D model of Røising *et al.* [62], the TRSB  $d_{xz \pm iyz}$  of Zutic and Mazin [16,65], or the newest  $d + ig$  proposal by Kivelson *et al.* [63].

The smaller  $\chi_0(0)/\chi_0(n) = 0.29 \pm 0.15$  for nodal states is compatible with even-parity order parameters with deep minima or nodes in the gap, listed above, particularly if other (impurity or orbital) contributions are included in our estimated  $\chi_0$ , which are not due to quasiparticle excitations [42,66,67]. The nodal  $s'$ - and  $d_{x^2-y^2}$ -wave states are supported by thermal conductivity [68], angle-dependent specific heat [43], penetration depth [69], and quasiparticle interference experiments [70], albeit not by the evidence of TRSB or by the recently observed discontinuity in the  $c_{66}$  shear modulus [71]. Future PNS measurements at lower fields and other field directions will place further constraints on the allowed paired states.

The authors are grateful for helpful discussions with J. F. Annett, S. E. Brown, K. Ishida, A. T. Rømer, and S. Yonezawa. Work is supported by the Engineering and Physical Sciences Research Council (EPSRC) Grant No. EP/R011141/1, the Centre for Doctoral Training in Condensed Matter Physics (EPSRC Grant No. EP/L015544/1), Japan Society for the Promotion of Science (JSPS) Kakenhi (Grants No. JP15H5852 and No. JP15K21717) and the JSPS-EPSRC Core-to-Core Program “Oxide-Superspin (OSS).”

\* a.petsch@bristol.ac.uk

† s.hayden@bristol.ac.uk

- [1] Y. Maeno, H. Hashimoto, K. Yoshida, S. Nishizaki, T. Fujita, J. G. Bednorz, and F. Lichtenberg, *Nature (London)* **372**, 532 (1994).
- [2] T. M. Rice and M. Sigrist, *J Phys. Condens. Matter* **7**, L643 (1995).
- [3] I. I. Mazin and D. J. Singh, *Phys. Rev. Lett.* **79**, 733 (1997).
- [4] A. P. Mackenzie and Y. Maeno, *Rev. Mod. Phys.* **75**, 657 (2003).
- [5] Y. Maeno, S. Kittaka, T. Nomura, S. Yonezawa, and K. Ishida, *J. Phys. Soc. Jpn.* **81**, 011009 (2012).
- [6] G. M. Luke, Y. Fudamoto, K. M. Kojima, M. I. Larkin, J. Merrin, B. Nachumi, Y. J. Uemura, Y. Maeno, Z. Q. Mao, Y. Mori, H. Nakamura, and M. Sigrist, *Nature (London)* **394**, 558 (1998).
- [7] K. Ishida, H. Mukuda, Y. Kitaoka, K. Asayama, Z. Q. Mao, Y. Mori, and Y. Maeno, *Nature (London)* **396**, 658 (1998).
- [8] J. A. Duffy, S. M. Hayden, Y. Maeno, Z. Q. Mao, J. Kulda, and G. J. McIntyre, *Phys. Rev. Lett.* **85**, 5412 (2000).
- [9] J. Xia, Y. Maeno, P. T. Beyersdorf, M. M. Fejer, and A. Kapitulnik, *Phys. Rev. Lett.* **97**, 167002 (2006).
- [10] A. P. Mackenzie, T. Scaffidi, C. W. Hicks, and Y. Maeno, *npj Quantum Mater.* **2**, 40 (2017).
- [11] J. R. Kirtley, C. Kallin, C. W. Hicks, E.-A. Kim, Y. Liu, K. A. Moler, Y. Maeno, and K. D. Nelson, *Phys. Rev. B* **76**, 014526 (2007).
- [12] C. W. Hicks, J. R. Kirtley, T. M. Lippman, N. C. Koshnick, M. E. Huber, Y. Maeno, W. M. Yuhasz, M. B. Maple, and K. A. Moler, *Phys. Rev. B* **81**, 214501 (2010).
- [13] P. J. Curran, V. V. Khotkevych, S. J. Bending, A. S. Gibbs, S. L. Lee, and A. P. Mackenzie, *Phys. Rev. B* **84**, 104507 (2011).
- [14] P. J. Curran, S. J. Bending, W. M. Desoky, A. S. Gibbs, S. L. Lee, and A. P. Mackenzie, *Phys. Rev. B* **89**, 144504 (2014).
- [15] H. Murakawa, K. Ishida, K. Kitagawa, Z. Q. Mao, and Y. Maeno, *Phys. Rev. Lett.* **93**, 167004 (2004).
- [16] I. Zutic and I. Mazin, *Phys. Rev. Lett.* **95**, 217004 (2005).
- [17] B. Kim, S. Khmelevskiy, I. I. Mazin, D. F. Agterberg, and C. Franchini, *npj Quantum Mater.* **2**, 37 (2017).
- [18] A. Pustogow, Y. Luo, A. Chronister, Y.-S. Su, D. A. Sokolov, F. Jerzembeck, A. P. Mackenzie, C. W. Hicks, N. Kikugawa, S. Raghu, E. D. Bauer, and S. E. Brown, *Nature (London)* **574**, 72 (2019).
- [19] K. Ishida, M. Manago, K. Kinjo, and Y. Maeno, *J. Phys. Soc. Jpn.* **89**, 034712 (2020).
- [20] K. Yosida, *Phys. Rev.* **110**, 769 (1958).
- [21] H. Won and K. Maki, *Phys. Rev. B* **49**, 1397 (1994).
- [22] A. J. Leggett, *Rev. Mod. Phys.* **47**, 331 (1975).
- [23] J. F. Annett, *Adv. Phys.* **39**, 83 (1990).
- [24] E. Pavarini and I. I. Mazin, *Phys. Rev. B* **74**, 035115 (2006).
- [25] Y. Luo, A. Pustogow, P. Guzman, A. P. Dioguardi, S. M. Thomas, F. Ronning, N. Kikugawa, D. A. Sokolov, F. Jerzembeck, A. P. Mackenzie, C. W. Hicks, E. D. Bauer, I. I. Mazin, and S. E. Brown, *Phys. Rev. X* **9**, 021044 (2019).
- [26] T. Oguchi, *Phys. Rev. B* **51**, 1385 (1995).
- [27] C. G. Shull and F. A. Wedgwood, *Phys. Rev. Lett.* **16**, 513 (1966).
- [28] J. Boucherle, J. Henry, R. J. Papoular, J. Rossat-Mignod, J. Schweizer, F. Tasset, and G. Uimin, *Physica (Amsterdam)* **192B**, 25 (1993).

- [29] C. Lester, J.-H. Chu, J. G. Analytis, A. Stunault, I. R. Fisher, and S. M. Hayden, *Phys. Rev. B* **84**, 134514 (2011).
- [30] J. Brand, A. Stunault, S. Wurmehl, L. Harnagea, B. Büchner, M. Meven, and M. Braden, *Phys. Rev. B* **89**, 045141 (2014).
- [31] A. M. Clogston, A. C. Gossard, V. Jaccarino, and Y. Yafet, *Phys. Rev. Lett.* **9**, 262 (1962).
- [32] R. M. White, *Quantum Theory of Magnetism* (Springer, Berlin, 1983).
- [33] R. J. Noer and W. D. Knight, *Rev. Mod. Phys.* **36**, 177 (1964).
- [34] I. Garifullin, N. Garifyanov, R. Salikhov, and L. Tagirov, *JETP Lett.* **87**, 316 (2008).
- [35] C. Caroli, P. G. D. Gennes, and J. Matricon, *Phys. Lett.* **9**, 307 (1964).
- [36] G. E. Volovik, *JETP Lett.* **58**, 469 (1993).
- [37] Z. Q. Mao, Y. Maeno, and H. Fukazawa, *Mater. Res. Bull.* **35**, 1813 (2000).
- [38] See details of the experiment at <https://doi.ill.fr/10.5291/ILL-DATA.DIR-183>.
- [39]  $M(\mathbf{G})$  includes the effect of the magnetic form factor. The spin-orbit interaction is negligible [72] and nuclear polarization [52] or ordering contributions have been neglected.
- [40] P. J. Brown, *International Tables for Crystallography Vol. C* (Kluwer, Dordrecht, 1992), p. 391.
- [41] P. W. Anderson and P. Morel, *Phys. Rev.* **123**, 1911 (1961).
- [42] See Supplemental Material at <http://link.aps.org/supplemental/10.1103/PhysRevLett.125.217004> for discussion of orbital contributions to the susceptibility, polarized neutron scattering and NMR knight shift measurements, Fermi liquid corrections, two-fluid model, and statistical analysis of previous data of Duffy *et al.*, which includes Refs. [8,18,19,40,43–54].
- [43] S. Kittaka, S. Nakamura, T. Sakakibara, N. Kikugawa, T. Terashima, S. Uji, D. A. Sokolov, A. P. Mackenzie, K. Irie, Y. Tsutsumi, K. Suzuki, and K. Machida, *J. Phys. Soc. Jpn.* **87**, 093703 (2018).
- [44] P. Coleman, *Introduction to Many-Body Physics* (Cambridge University Press, Cambridge, England, 2015).
- [45] M. Kim, J. Mravlje, M. Ferrero, O. Parcollet, and A. Georges, *Phys. Rev. Lett.* **120**, 126401 (2018).
- [46] A. Tamai, M. Zingl, E. Rozbicki, E. Cappelli, S. Riccò, A. de la Torre, S. M. Walker, F. Bruno, P. King, W. Meevasana, M. Shi, M. Radović, N. Plumb, A. Gibbs, A. Mackenzie, C. Berthod, H. Strand, M. Kim, A. Georges, and F. Baumberger, *Phys. Rev. X* **9**, 021048 (2019).
- [47] Y. Maeno, K. Yoshida, H. Hashimoto, S. Nishizaki, S.-i. Ikeda, M. Nohara, T. Fujita, A. P. Mackenzie, N. E. Hussey, J. G. Bednorz, and F. Lichtenberg, *J. Phys. Soc. Jpn.* **66**, 1405 (1997).
- [48] S. Nishizaki, Y. Maeno, and Z. Mao, *J. Phys. Soc. Jpn.* **69**, 572 (2000).
- [49] I. I. Mazin and R. E. Cohen, *Ferroelectrics* **194**, 263 (1997).
- [50] A. J. Leggett, *Phys. Rev. Lett.* **14**, 536 (1965).
- [51] C. G. Shull and R. P. Ferrier, *Phys. Rev. Lett.* **10**, 295 (1963).
- [52] Y. Ito and C. G. Shull, *Phys. Rev.* **185**, 961 (1969).
- [53] W. H. Press, B. P. Flannery, S. A. Teukolsky, and W. T. Vetterling, *Numerical Recipes in FORTRAN 77*, 2nd ed. (Cambridge University Press, Cambridge, England, 1993), Vol. 1.
- [54] A. Chronister, A. Pustogow, N. Kikugawa, D. A. Sokolov, F. Jerzembeck, C. W. Hicks, A. P. Mackenzie, E. D. Bauer, and S. E. Brown, [arXiv:2007.13730](https://arxiv.org/abs/2007.13730).
- [55] M. W. Haverkort, I. S. Elfimov, L. H. Tjeng, G. A. Sawatzky, and A. Damascelli, *Phys. Rev. Lett.* **101**, 026406 (2008).
- [56] C. Noce and M. Cuoco, *Phys. Rev. B* **59**, 2659 (1999).
- [57] K. Deguchi, M. A. Tanatar, Z. Mao, T. Ishiguro, and Y. Maeno, *J. Phys. Soc. Jpn.* **71**, 2839 (2002).
- [58] S. Kittaka, A. Kasahara, T. Sakakibara, D. Shibata, S. Yonezawa, Y. Maeno, K. Tenya, and K. Machida, *Phys. Rev. B* **90**, 220502(R) (2014).
- [59] Y. Amano, M. Ishihara, M. Ichioka, N. Nakai, and K. Machida, *Phys. Rev. B* **91**, 144513 (2015).
- [60] The available form factor  $Ru^+$  was used.
- [61] A. T. Rømer, D. D. Scherer, I. M. Eremin, P. J. Hirschfeld, and B. M. Andersen, *Phys. Rev. Lett.* **123**, 247001 (2019).
- [62] H. S. Røising, T. Scaffidi, F. Flicker, G. F. Lange, and S. H. Simon, *Phys. Rev. Research* **1**, 033108 (2019).
- [63] S. A. Kivelson, A. C. Yuan, B. Ramshaw, and R. Thomale, *npj Quantum Mater.* **5**, 43 (2020).
- [64] G. Baskaran, *Physica (Amsterdam)* **223–224B**, 490 (1996).
- [65] H. G. Suh, H. Menke, P. M. R. Brydon, C. Timm, A. Ramires, and D. F. Agterberg, *Phys. Rev. Research* **2**, 032023 (2020).
- [66] A. A. Abrikosov and L. P. Gor'kov, *Sov. Phys. JETP* **15**, 752 (1962).
- [67] Y. Bang, *Phys. Rev. B* **85**, 104524 (2012).
- [68] E. Hassinger, P. Bourgeois-Hope, H. Taniguchi, S. René de Cotret, G. Grissonnanche, M. S. Anwar, Y. Maeno, N. Doiron-Leyraud, and L. Taillefer, *Phys. Rev. X* **7**, 011032 (2017).
- [69] I. Bonalde, B. D. Yanoff, M. B. Salamon, D. J. Van Harlingen, E. M. E. Chia, Z. Q. Mao, and Y. Maeno, *Phys. Rev. Lett.* **85**, 4775 (2000).
- [70] R. Sharma, S. D. Edkins, Z. Wang, A. Kostin, C. Sow, Y. Maeno, A. P. Mackenzie, J. C. S. Davis, and V. Madhavan, *Proc. Natl. Acad. Sci. U.S.A.* **117**, 5222 (2020).
- [71] S. Ghosh, A. Shekhter, F. Jerzembeck, N. Kikugawa, D. A. Sokolov, M. Brando, A. P. Mackenzie, C. W. Hicks, and B. J. Ramshaw, *Nat. Phys.* (2020), <https://doi.org/10.1038/s41567-020-1032-4>.
- [72] C. G. Shull, *Phys. Rev. Lett.* **10**, 297 (1963).